Molecular Therapy
Methods & Clinical Development
Original Article

A Novel Gene Therapy Approach for GSD III Using an AAV Vector Encoding a Bacterial Glycogen Debranching Enzyme

Jeong-A Lim,[1] Su Jin Choi,[1] Fengqin Gao,[1] Priya S. Kishnani,[1] and Baodong Sun[1]

[1]Division of Medical Genetics, Department of Pediatrics, Duke University School of Medicine, Durham, NC, USA

Glycogen storage disease type III (GSD III) is an inherited disorder caused by a deficiency of glycogen debranching enzyme (GDE), which results in the accumulation of abnormal glycogen (limit dextrin) in the cytoplasm of liver, heart, and skeletal muscle cells. Currently, there is no curative treatment for this disease. Gene therapy with adeno-associated virus (AAV) provides an optimal treatment approach for monogenic diseases like GSD III. However, the 4.6 kb human GDE cDNA is too large to be packaged into a single AAV vector due to its small carrying capacity. To overcome this limitation, we tested a new gene therapy approach in GSD IIIa mice using an AAV vector ubiquitously expressing a smaller bacterial GDE, Pullulanase, whose cDNA is 2.2 kb. Intravenous injection of the AAV vector (AAV9-CB-Pull) into 2-week-old GSD IIIa mice blocked glycogen accumulation in both cardiac and skeletal muscles, but not in the liver, accompanied by the improvement of muscle functions. Subsequent treatment with a liver-restricted AAV vector (AAV8-LSP-Pull) reduced liver glycogen content by 75% and reversed hepatic fibrosis while maintaining the effect of AAV9-CB-Pull treatment on heart and skeletal muscle. Our results suggest that AAV-mediated gene therapy with Pullulanase is a possible treatment for GSD III.

INTRODUCTION

Mutations in the *AGL* gene cause deficiency of glycogen debranching enzyme (GDE), leading to glycogen storage disease type III (GSD III, also known as Cori's disease). In mammals and yeast, GDE is a bifunctional enzyme that helps breakdown glycogen via two separate enzyme activities, 4-α-D-glucanotransferase (EC 2.4.1.25) and amylo-α-1,6-glucosidase (EC 3.2.1.33), both encoded by the same gene.[1–3] Glycogen phosphorylase initiates glycogenolysis process by releasing glucose-1-phosphate from branches of glycogen molecules until it reaches four residues to the branching points. GDE then transfers three of the remaining four glucose units to the end of a nearby branch and exposes the α(1→6) branching point where GDE can hydrolyze the α(1→6) linkage to release a glucose molecule via its amylo-α-1,6-glucosidase activity. Due to the impairment of the GDE activities in GSD III, abnormal glycogen with short outer branches (limit dextrin) accumulates in multiple tissues, primarily in the liver, heart, and skeletal muscle. Most patients (about 85%) have both muscle and liver involvement (type IIIa), while others (about 15%) have disease limited to liver (type IIIb).[4–6] In infancy and early childhood, the disease manifests with mostly liver involvement: hepatomegaly, hypoglycemia, hyperlipidemia, and elevated hepatic transaminases.[4,7] In adolescence and adulthood, these liver manifestations seem to become less pronounced, but progressive liver fibrosis and hepatic failure can occur, and some of the patients may develop end-stage liver cirrhosis, hepatic adenoma, or hepatocellular carcinomas.[4,7–9] Muscle symptoms normally escalate in adulthood of GSD IIIa patients.[4,7] Muscle weakness and muscle wasting can occur progressively and most patients exhibit exercise intolerance.[6,7,10–12] In some cases, cardiomyopathy can lead to heart failure and sudden death.[4,7,13] Bulbar muscle weakness was seen in some GSD IIIa patients.[14]

To date, there is no cure for GSD III. Current treatments rely on symptomatic and dietary management to control blood glucose levels.[7] Because GSD III is a single gene disorder, it is a suitable candidate for adeno-associated virus (AAV)-mediated gene therapy. However, a gene expression cassette containing the large 4.6 kb human GDE cDNA, a promoter, and a poly(A) (polyadenylation) signal sequence cannot be packaged into a single AAV capsid, whose carrying capacity is less than 4.7 kb. In this study, we tested a novel gene therapy using an AAV vector expressing a smaller bacterial GDE, Pullulanase (type I, EC 3.2.1.41) derived from *Bacillus subtilis* strain 168 in our recently generated GSD IIIa mouse model. Unlike human GDE, Pullulanase encoded by the *amyX* gene has only amylo-α-1,6-glucosidase activity and can directly cleaves the α(1→6) bonds at the branching points in limit dextrin to release maltotetraose molecules, without a need of transferring three glucose residues.[15] The cDNA of this enzyme is only 2.2 kb, small enough for efficient AAV packaging.

Here, for the first time, we showed that AAV-mediated Pullulanase expression cleared abnormal glycogen accumulation in the liver and muscles and improved liver and muscle functions in GSD IIIa

Received 17 January 2020; accepted 27 May 2020;
https://doi.org/10.1016/j.omtm.2020.05.034.

Correspondence: Baodong Sun, Division of Medical Genetics, Department of Pediatrics, Duke University School of Medicine, Durham, NC, USA.
E-mail: baodong.sun@duke.edu

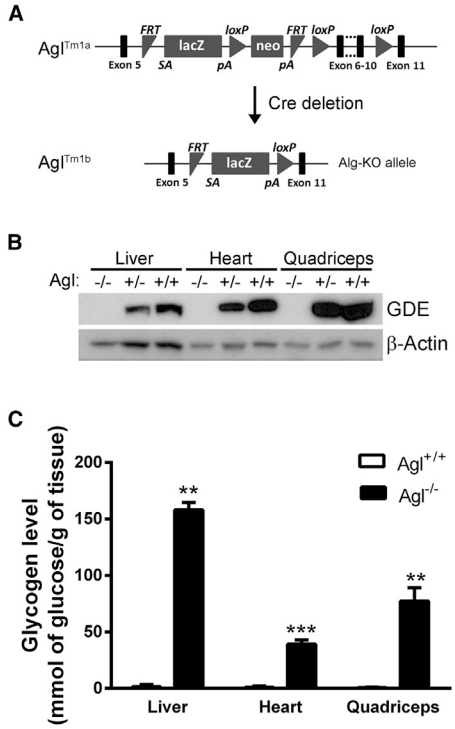

Figure 1. Generation of a Mouse Model of GSD IIIa

(A) Generation of heterozygous $Agl^{+/-}$ mice by crossing the Agl^{Tm1a} mice with CMV-Cre mice. Homozygous $Agl^{-/-}$ mice were used as breeders to produce GSD IIIa (*Agl* knockout) mice. (B) Western blot with an anti-GDE antibody confirmed the absence of GDE protein in tissues of GSD IIIa ($Agl^{-/-}$) mice. β-Actin was used as a loading control. (C) Glycogen levels were measured in the liver, heart, and quadriceps from 3-month-old GSD IIIa ($Agl^{-/-}$) and WT ($Agl^{+/+}$) mice. Glycogen contents were significantly higher in all the tested tissues of GSD IIIa mice than those of the WT mice. The graph represents the mean ± SD n = 4 for WT and n = 5 for GSD IIIa mice. Student's t test. ***$p < 0.001$ and **$p < 0.01$.

mice. These results suggest that Pullulanase is a therapeutic candidate for GSD III gene therapy with AAV.

RESULTS

GSD IIIa Mouse Model Replicates the Disease Phenotype of Human Patients

We generated a GSD IIIa (*Agl* knockout [KO], $Agl^{-/-}$) mouse model by deleting exons 6 to 10 in the *Agl* gene (Figure 1A). Western blot confirmed the absence of GDE protein in the liver, heart, and skeletal muscle (quadriceps) of GSD IIIa ($Agl^{-/-}$) mice (Figure 1B). Glycogen accumulation was observed profoundly in the liver, heart, skeletal muscles (quadriceps, gastrocnemius, soleus, diaphragm, and tongue) and smooth muscle (bladder), moderately in the heart, in some regions of the brain and spinal cord of the untreated GSD IIIa mice at 3 months of age (Figures 1C, 3A, 3B, and 4). In addition, our GSD IIIa mouse model showed symptoms of liver and skeletal muscle defects similar to human GSD IIIa patients, such as liver fibrosis (Figure 3C), hepatomegaly (Figure 5A), increased plasma alanine aminotransferase (ALT) activity (Figure 5B), elevated disease urinary Glc4 (Figure 5C), and impaired muscle functions (Figure 5D).

AAV-Mediated Pullulanase Expression in Liver and Muscle Tissues of GSD IIIa Mice

We optimized the codons of Pullulanase coding sequence (Figure S1) for expression in human cells and sub-cloned it into a mammalian expression vector pcDNA3.1(+), to generate pcDNA3.1-Pull. Expression of Pullulanase was verified by western blot and enzyme activity assay in the vector transfected HEK293T cells; in contrast, no Pullulanase expression was detected in the untreated cells (Figure S2).

Because GSD III manifests mainly in liver, heart, and skeletal muscles,[7] we focused our study on these tissues. AAV vector plasmids carrying the codon-optimized Pullulanase (Pull) under the control of the ubiquitous CMV enhancer/chicken β-actin promoter (pAAV-CB-Pull) and the liver-specific promoter (pAAV-LSP-Pull) were constructed (Figure 2A). These two vectors were packaged into AAV9 (AAV9-CB-Pull) and AAV8 (AAV8-LSP-Pull), respectively. 2-week-old GSD IIIa mice were treated with AAV9-CB-Pull (1×10^{13} vg/kg). After 10 weeks, half of the mice were sacrificed to evaluate the efficacy of AAV9-CB-Pull treatment in different tissues at 3 months of age (Figure 2B, 3 months, gray arrow) and the other half were further treated with AAV8-LSP-Pull (1×10^{13} vg/kg) for another 10 weeks to correct liver abnormalities (Figure 2B, 5 months, black arrow). Behavioral tests were performed to evaluate muscle functions during the treatments at 2, 2.5, 3, 4, and 5 months old age (Figure 2B, open arrows).

To determine whether AAV treatment caused an early underlying liver toxicity, we analyzed ALT and aspartate aminotransferase (AST) activities in the plasma at 7 and 14 days post vector injection. Neither ALT nor AST activity significantly increased in the AAV9-CB-Pull-treated mice compared with that in the untreated GSD IIIa mice (Figure S3). To evaluate the transduction efficiency of the AAV vectors in liver and muscles, we checked AAV genome copy numbers using real-time PCR and protein expression by western blot. 10 weeks after the AAV9-CB-Pull (CB) treatment, AAV copy numbers were high in the heart (8.69 ± 2.22 vg/genome) and low in the quadriceps (0.68 ± 0.15) and liver (0.40 ± 0.32; Figure 2C). Protein level was high in the heart, moderate in the quadriceps, and undetectable in the liver (Figure 2D). Consistent with the western blot results, Pullulanase enzyme activity was profoundly high in the heart (33.77 ± 8.51 mU/mg) and readily detectable in the quadriceps (6.64 ± 2.11 mU/mg) but undetectable in the liver at 3 months of age (Figure 2E). However, 10 weeks after the secondary treatment with AAV8-LSP-Pull (CB+LSP), the AAV genome copy number, protein expression, and enzyme activity were all significantly increased in the liver (Figures 2C–2E, black bars); enzyme activity was lowered in the heart (18.69 ± 6.19 mU/mg) and still detectable in the skeletal muscle (Figure 2E, black bars).

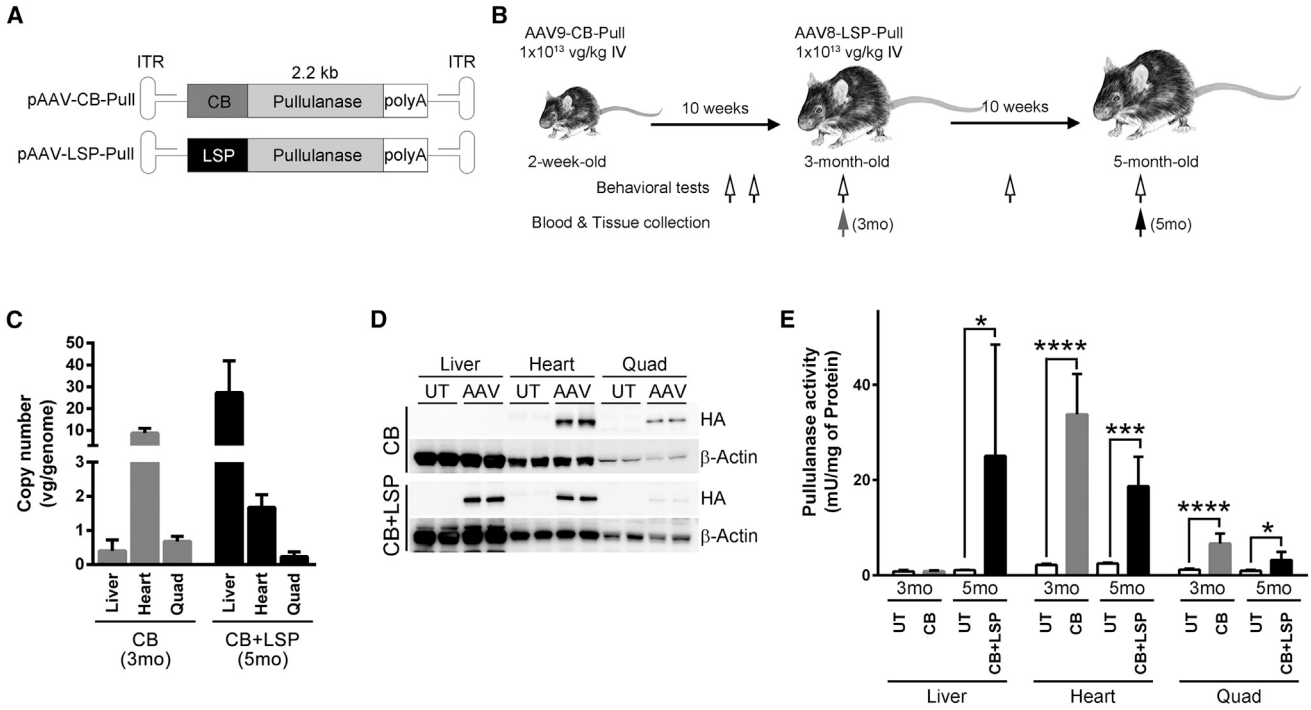

Figure 2. AAV-Mediated Gene Delivery of Pullulanase in the Liver and Muscles of GSD IIIa Mice

(A) The diagram shows the constructs of AAV vector containing the 2.2 kb codon-optimized Pullulanase cDNA under the control of the ubiquitous CMV enhancer/chicken β-actin promoter (CB) and the liver-specific promoter (LSP). ITR, inverted terminal repeats; poly(A), human growth hormone polyadenylation signal sequence. (B) Experimental flow chart of AAV treatments in GSD IIIa mice. Fifteen mice were injected with AAV9-CB-Pull at 2 weeks of age at a dose of 1×10^{13} vg/kg. Eight mice were sacrificed after 10 weeks of treatment (3 months old, gray arrow) for sample collection; the remaining seven mice received a second AAV injection with AAV8-LSP-Pull at the same dose. Tissues and plasma were analyzed after another 10 weeks (5 months old, black arrow). Behavioral tests were performed at ages 2, 2.5, 3, 4, and 5 months old (open arrows). (C) AAV genome copy numbers were determined by real-time PCR using gene-specific primers for Pullulanase (see Materials and Methods). The copy number was high in the heart and low in the liver and skeletal muscle of the AAV9-CB-Pull-treated mice at 3 months of age (CB, gray). 10 weeks after subsequent AAV8-LSP-Pull treatment (CB+LSP, black), the AAV copy number profoundly increased in the liver. The graph represents the mean ± SD n = 5 for each group. vg/genome, vector genome copies per nucleus (genome). (D) Western blot analysis using an anti-HA antibody confirmed the expression of Pullulanase in tissues of the AAV-treated GSD IIIa mice. Pullulanase was undetectable in any tissues of the untreated (UT) mice. Pullulanase was not detectable in the liver of the CB-treated mice but was highly expressed in the liver of CB+LSP-treated mice. The heart showed a high level and skeletal muscle showed a low level (but detectable) of Pullulanase in both CB- and CB+LSP-treated mice. β-Actin was used as a loading control. (E) Pullulanase activity was evaluated in the liver, heart, and skeletal muscle using the Pullulanase activity kit (Megazyme). Consistent with the western blot results, the enzyme activity was not detectable in the CB-treated liver but drastically increased in the CB+LSP-treated liver. The enzyme activity was significantly elevated in the heart and skeletal muscle of both CB- and CB+LSP-treated mice compared to the UT mice. The graph represents the mean ± SD n = 5 for UT, n = 8 for CB, and n = 7 for CB+LSP; Student's t test. *$p < 0.05$, ***$p < 0.001$, and ****$p < 0.0001$.

Pullulanase Reduced Glycogen Accumulation in the Liver and Muscles and Reversed Liver Fibrosis in GSD IIIa Mice

Since glycogen accumulation in tissues is the primary phenotype of GSD III, we compared glycogen levels in the liver, heart, and skeletal muscle of the untreated and AAV-treated GSD IIIa mice. Both the CB and CB+LSP combination treatments significantly decreased glycogen contents in the heart (−75%~80%) and skeletal muscle (−80%) compared to those in the untreated mice (Figure 3A). As expected, glycogen level did not change significantly in the CB-treated liver but decreased remarkably (−75%) in the CB+LSP-treated liver (Figure 3A).

Periodic acid-Schiff (PAS) staining of tissue sections confirmed the glycogen content results. CB treatment effectively cleared glycogen accumulation in the heart and skeletal muscles (quadriceps, gastrocnemius, soleus, diaphragm, and tongue), but had no effect on the liver, smooth muscle (bladder), brain (cerebellum), or the spinal cord (Figures 3B and 4, CB). Additional treatment with the second AAV8-LSP-Pull vector cleared glycogen accumulation in the liver (Figure 3B, CB+LSP).

Another hepatic disease manifestation in GSD III is progressive liver fibrosis, which has been shown in our previous reported canine GSD IIIa model.[16] We evaluated the liver fibrosis status in the untreated and AAV-treated GSD IIIa mice by trichrome staining. Untreated GSD IIIa liver showed similar early stage (stage 1–2) fibrosis with appearance of blue on staining at both 3 and 5 months of age (Figure 3C, white arrows). The early (on postnatal day 14) treatment with AAV9-CB-Pull, which did not change the glycogen level in the liver, did not prevent liver fibrosis

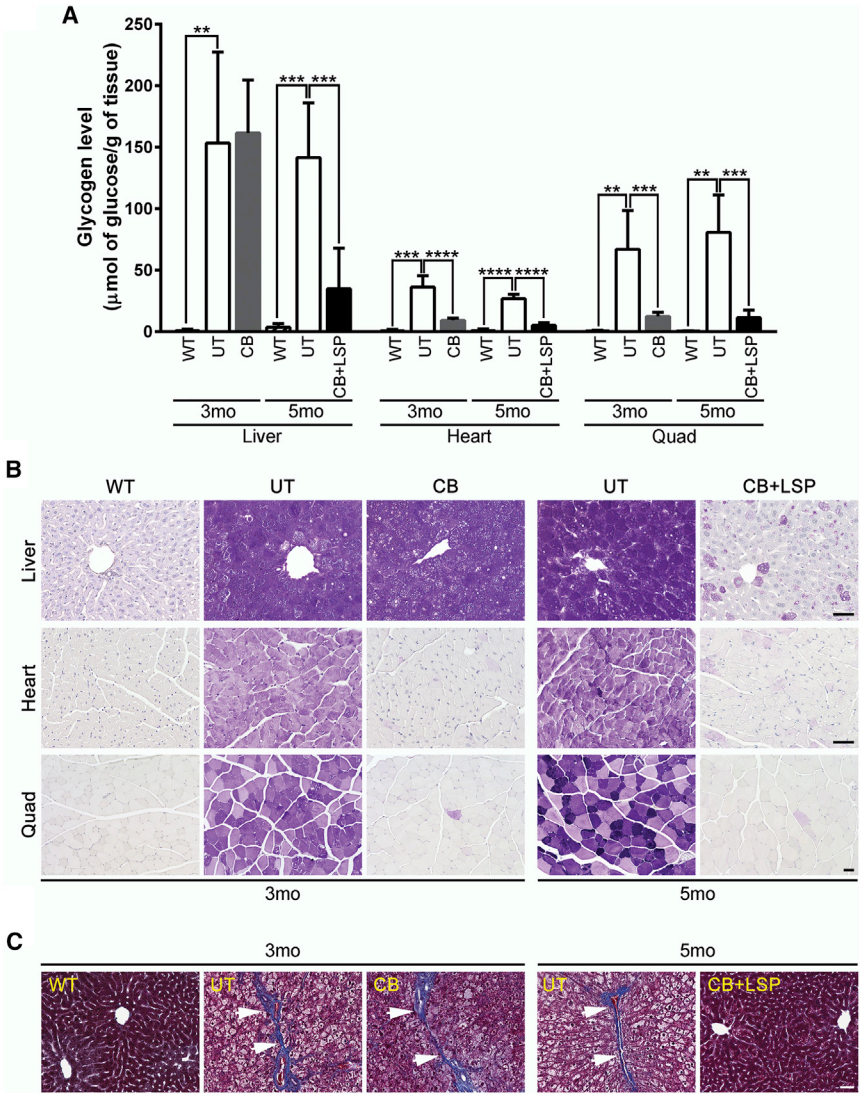

Figure 3. Pullulanase Reduced Glycogen Accumulation in the Liver and Muscles and Reversed Liver Fibrosis in GSD IIIa Mice

(A) Glycogen contents were measured in the liver, heart, and skeletal muscle. Consistent with the enzyme activity results, there is no difference in liver glycogen content between the UT- and CB-treated GSD IIIa mice at 3 months of age, but glycogen level was reduced significantly in the CB+LSP-treated liver at 5 months of age. Glycogen content was profoundly decreased in the heart and skeletal muscle of both CB- and CB+LSP-treated mice. The graph represents the mean ± SD n = 4 for WT, n = 5 for UT, n = 8 for CB, and n = 7 for CB+LSP; Student's t test. **p < 0.01, ***p < 0.001, and ****p < 0.0001. (B) Periodic acid-Schiff (PAS) staining was used for detection of glycogen accumulation in tissues. Untreated GSD IIIa mice showed intense PAS-positive glycogen accumulation (purple) in the liver, heart, and skeletal muscle. CB treatment had no effect on liver glycogen accumulation; in contrast, CB+LSP treatment markedly reduced glycogen accumulation in the liver. Glycogen buildup was profoundly cleared in the heart and skeletal muscle by both CB and CB+LSP treatments. At least 3 mice were examined in each group, and representative images are shown. Scale bar, 50 μm. (C) Trichrome staining was used for detection of liver fibrosis. The blue staining (arrows) indicates the presence of fibrotic tissues in the liver of UT- and CB-treated GSD IIIa mice. CB+LSP treatment successfully reversed liver fibrosis. At least 3 mice were examined in each group, and representative images are shown. Scale bar, 50 μm.

(Figure 3C). There were no obvious fibrotic tissues in the CB+LSP-treated liver (Figure 3C), suggesting that the secondary AAV8-LSP-Pull treatment can reverse and prevent early stage liver fibrosis in adult GSD IIIa mice.

Pullulanase Normalized Disease Symptoms and Improved Muscle Functions in GSD IIIa Mice

Hepatomegaly is one of the most common symptoms of GSD III patients.[4,7] Therefore, we measured the liver size using the liver-to-bodyweight ratio. As we expected, the liver-to-bodyweight ratio clearly increased in the untreated GSD IIIa mice (7%~8%) compared to wild-type (WT) level (about 4%; Figure 5A). Consistent with the Pullulanase activity and glycogen data, the liver size remained unchanged in the CB-treated mice but was normalized to the WT level in the CB+LSP-treated mice (Figure 5A). Furthermore, the activity of ALT in the plasma, which is commonly used for monitoring liver damage, was reduced to the WT level in CB+-LSP-treated mice (Figure 5B). The CB-treated mice showed a slightly decreased in plasma ALT activity compared with the untreated mice at 3 months of age (p = 0.09, Figure 5B). A significant increase in plasma ALT level in the untreated GSD IIIa mice from 3 months of age (264.0 ± 153.4 U/L) to 5 months of age (744.0 ± 170.4 U/L) suggests progressive liver damage during that time (Figure 5B).

Urinary Glc4, a known disease biomarker for Pompe disease (GSD II) that is often correlated with the levels of glycogen accumulation in skeletal muscle,[17] has been indicated as a potential biomarker for GSD III.[7,18,19] The concentration of urinary Glc4 was reduced to the WT level in the CB-treated GSD IIIa mice at 3 months of age (Figure 5C). The behavioral tests including treadmill, inverted wire hang, and Rota-rod have been broadly used for assessment of muscle function in mice.[20–22] After AAV treatments, all the three tests showed significant improvement of muscle function (Figure 5D). Notably, the running distance improved dramatically in the treadmill test after AAV treatments (Figure 5D).

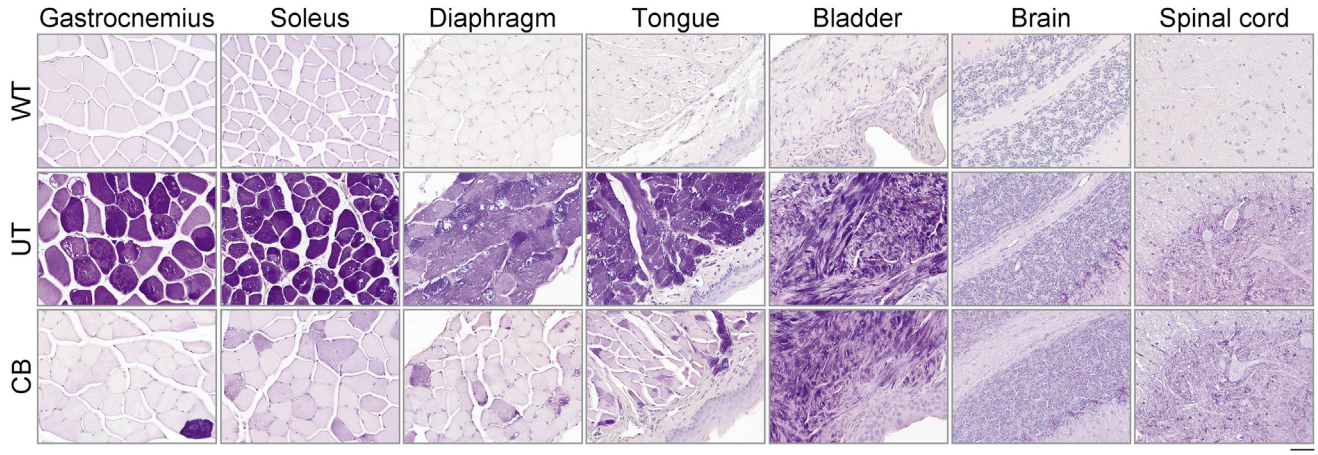

Figure 4. AAV-CB-Pull Treatment Reduced Glycogen Accumulation in the Skeletal Muscles but Not in Smooth Muscle or the CNS of GSD IIIa Mice
Glycogen level was assessed by PAS staining in tissues of WT mice and UT- and CB-treated GSD IIIa mice at 3 months of age. Untreated GSD IIIa mice showed massive glycogen staining in the skeletal muscles (gastrocnemius, soleus, diaphragm, and tongue) and smooth muscle (bladder) and a mild but significant amount of glycogen accumulation in some regions of the brain (cerebellum) and spinal cord. CB treatment markedly reduced glycogen accumulation in all the skeletal muscles but had no effect on the smooth muscle, brain, and spinal cord. At least 3 mice were examined in each group, and representative images are shown. Scale bar, 50 μm.

DISCUSSION

GSD III is a rare (estimated at 1 in every 100,000 births) inherited disorder characterized by the accumulation of limit dextrin-like glycogen in liver and muscle tissues. Progressive liver cirrhosis and skeletal and cardiac myopathy are the major causes of morbidity and mortality in patients with GSD III.[7] Our GSD IIIa mouse model imitates the major haptic and muscular symptoms observed in human patients, such as hepatomegaly, progressive liver fibrosis, exercise intolerance, and impaired muscle function. Recently, several other *Agl*-KO mouse models were generated by other groups using a similar gene deletion strategy. Like our model, their *Agl*-KO mice also showed complete lack of GDE expression and increased glycogen accumulation in the liver, heart, and skeletal muscles, accompanied by the remarkable liver and muscle functional deficits.[23–25] Surprisingly, we did not see hypoglycemia in our GSD IIIa mice tested at age of 3 months even after 24 h fasting (data not shown). Similarly, Liu's model did not show hypoglycemia from ages of 4 weeks up to 40 weeks after 12 or 24 h fasting.[23] However, Pagliarani et al.[24] detected significant hypoglycemia in their 7- and 8-month-old *Agl*-KO mice and Vidal et al.[25] observed a significant reduction in blood glucose levels in their 6-month-old *Agl*-KO mice. The discrepancy in hypoglycemia between these murine models is likely a result of different strategies being used for *Agl* gene deletion and different ages being tested for blood work. The lack of hypoglycemia phenomenon in our GSD IIIa mice represents one limitation of this animal disease model.

Additionally, our GSD IIIa mouse model showed early glycogen accumulation in the cerebellum at a younger age (3 months) while the *Agl*-KO mouse model developed by Pagliarani et al.[24] showed that at a much older age (18 months). The pattern of glycogen distribution in the brain in our GSD IIIa mouse model is very similar to that observed in the GSD II mouse model, acid-α-glucosidase knockout (GAA-KO) showing that glycogen deposition was mostly detected in the granular cells and the Purkinje cell layer.[26] However, unlike the GAA-KO mice, we could not detect any unusual neurological behaviors in the 3- or 5-month-old GSD IIIa mice except the Rota-rod test, which evaluates motor coordination and balance, as well as skeletal muscle function. Since we could not observe other neurological abnormal behaviors, the shorter latency of GSD IIIa mice than the WT mice to fall in the Rota-rod test (Figure 5D) would be mostly related to skeletal muscle weakness. Furthermore, the improved performance in the Rota-rod test after Pullulanase treatments (Figure 5D) is most likely a result of skeletal muscle recovery because the treatment did not apparently affect the glycogen accumulation in the brain and spinal cord (Figure 4). Recently, the possibilities for psychopathological or neuropsychological impairment were suggested in GSD IIIa patients.[27] However, to confirm the neurological involvement in the disease, further studies on the natural history are needed either in a larger group of patients or animal models. We are monitoring whether aged GSD IIIa mice show neurological impairments.

Currently, there is no cure for this disease. Current treatments for GSD III are symptomatic and do not decelerate or prevent the progression of the disease. Dietary management using cornstarch to maintain euglycemia is recommended for patients with GSD III.[4,7] High-protein diet is also recommended to help ameliorate skeletal and cardiac myopathies.[4,7,28] Patients with severe cirrhosis or hepatocellular carcinoma are often considered for liver transplant.[4,7] A recent study showed that a glucose-free/high-protein diet improved skeletal muscle function and hepatomegaly in a GSD III mouse model.[29] Several preclinical studies using *in vitro* model and animal disease models have suggested potential treatments for GSD III. Enzyme therapy with recombinant human GAA (rhGAA, Alglucosidase alfa) reduced glycogen content in primary GSD IIIa patient muscle cells.[30] In a GSD IIIa canine model, daily rapamycin treatment

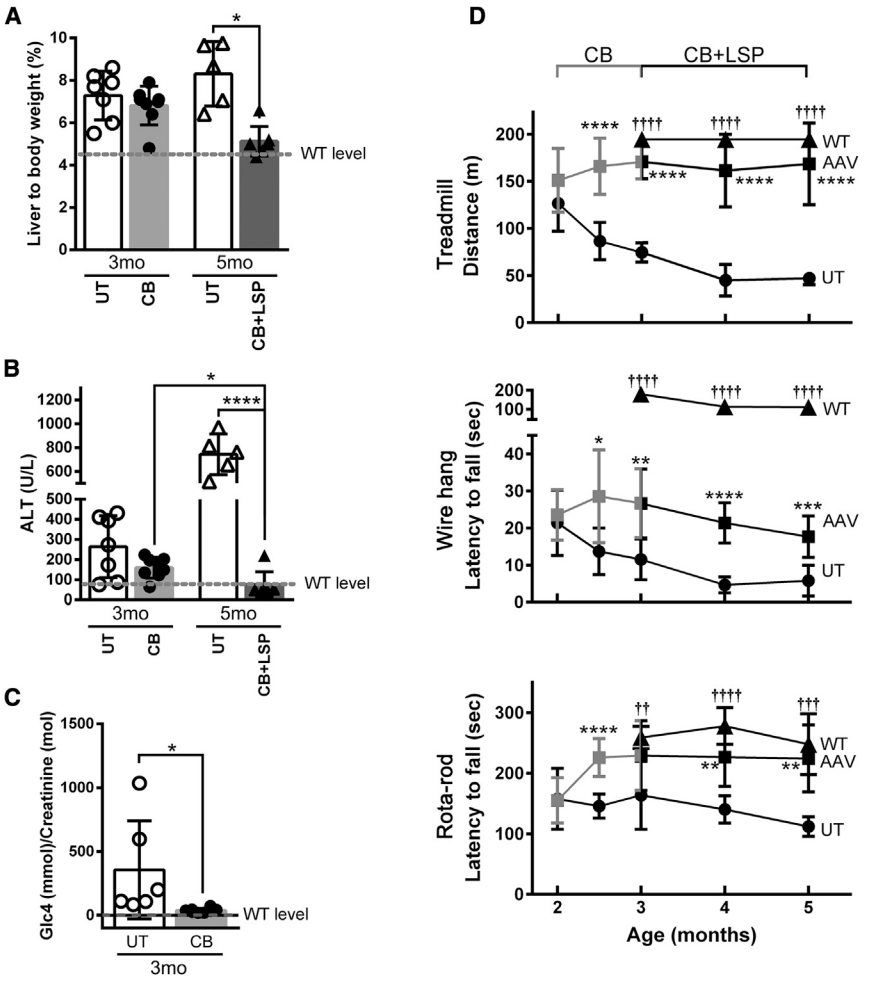

Figure 5. Pullulanase Normalized Disease Symptoms and Improved Muscle Function

(A) The ratio of liver to body weight was measured to determine hepatomegaly. The ratio did not change by the CB treatment. However, the liver size was significantly reduced by the CB+LSP treatment. The dotted line represents the level of liver to body weight ratio in WT mice (4.5% ± 0.2%, n = 6). The graph represents the mean ± SD n = 7 for UT (3 months) and CB+LSP, n = 8 for CB, and n = 5 for UT (5 months). Each dot/triangle represents an individual mouse. Student's t test. *p < 0.05. (B) The activity of alanine aminotransferase (ALT) was measured in the plasma from UT- and AAV-treated GSD IIIa mice to evaluate liver function. The ALT level was slightly reduced (p = 0.09) in the CB-treated mice compared to UT. The ALT level was remarkably increased in UT mice from age 3 to 5 months. CB+LSP treatment significantly reduced plasma ALT activity compared with UT mice. The graph represents the mean ± SD n = 7 for UT (3 months) and CB+LSP, n = 8 for CB, and n = 5 for UT (5 months). Each dot/triangle represents an individual mouse. The dotted line represents the ALT level in WT mice (98.1 ± 33.24 U/L, n = 4). Student's t test. *p < 0.05 and ****p < 0.0001. (C) The concentrations of urinary Glc4 were assessed in the UT and AAV-CB-Pull (CB)-treated GSD IIIa mice. The CB-treated mice showed a significant decrease in the level of urinary Glc4 compared to the UT mice. The urinary creatinine level was used for normalization. The graph represents the mean ± SD, n = 6 for UT and n = 8 for CB. Each dot represents an individual mouse. The dotted line represents the WT level (4.4 ± 1.7 mmol/mol of creatinine, n = 7). Student's t test. *p < 0.05. (D) Treadmill test was used for evaluating exercise intolerance in WT, UT-, and AAV-treated GSD IIIa mice. The graph represents the maximum running distance. The running distance gradually declined in the UT mice with time (UT, dots). However, the running distance was steady in the AAV-treated mice (AAV, squares). Wire hang test was used to assess limb muscle strength. The time of latency to fall was measured and the maximum time from three independent trials was used for comparison. The hanging time was also progressively decreased in UT mice with age (UT, dots), but AAV treatments significantly improved the hanging time (AAV, squares). Rota-rod test was used to measure muscle strength, motor coordination, and balance. The mice were tested during three sessions using the accelerating Rota-rod protocol (4.0–40.0 rpm), and the latency to fall was recorded. AAV-treated mice also showed significant improvement in Rota-rod performance compared to the UT mice. The data represents the mean ± SD, n = 5 for WT and n = 7 for both UT- and AAV-treated GSD IIIa mice. Student's t test. ††p < 0.01, †††p < 0.001, and ††††p < 0.0001, WT compared to UT. *p < 0.05, **p < 0.01, ***p < 0.001, and ****p < 0.0001, AAV compared to UT.

corrected glycogen accumulation in skeletal muscle and liver and effectively prevented liver fibrosis.[31] Pursell et al.[32] reported that silencing of liver glycogen synthase (GYS2) by RNAi prevented liver glycogen accumulation and liver fibrosis in a GSD III mouse model.

Since GSD III is a well-defined monogenic disorder, AAV-mediated gene therapy provides an optimal therapeutic approach for the disease. AAV8 and AAV9 are preferred gene therapy vectors for GSD III because both vectors can transduce liver and muscle tissues with high efficiency and have been evaluated in some clinical trials.[33–37] However, packaging of the large (4.6 kb) human GDE cDNA into a single AAV vector is impractical due to the small carrying capacity of AAV vector (less than 5 kb). To date, there is only one report of AAV-mediated gene replacement therapy for GSD III using a dual overlapping AAV vector system by splitting the human GDE cDNA into two halves and then packaging them into two separate AAV vectors.[25] Co-administration of the dual overlapping AAV vectors into GSD III mice resulted in GDE expression in the liver and muscle and reduced glycogen accumulation, rescued muscle strength, and improved blood glucose. However, the efficiency of reconstitution of the full-length protein is low and homologous recombination is not equally efficient in all tissues.[25]

In this study, we tested an innovative gene therapy approach using AAV vectors to express a smaller bacterial GDE in GSD IIIa mice. Pullulanase and human GDE both belong to glucoside hydrolase superfamily and the two proteins have similar 3D structures and carbohydrate binding regions in their N-terminal regions (Figure S4).

However, the overall sequence homology between the bacterial Pullulanase (GenBank: NP_390871.2) and human GDE (GenBank: NP_000019.2) is low (Figure S4). Therefore, Pullulanase-induced cytotoxic T cell response is highly predictable when treating human patients or GSD IIIa mice. In our previous study, we demonstrated that administration of an AAV vector containing the ubiquitous CB promoter (AAV-CB-hGAA) in GAA-KO mice at a young age (on postnatal day 14) successfully prevented human GAA-induced immune responses and corrected glycogen storage in all the affected tissues.[26] However, the fast growth rate of the liver in neonatal mice causes a rapid dilution and loss of the AAV vector over time, which makes this treatment approach less effective in the liver. For a proof-of-principle study, we treated 2-week-old GSD IIIa mice with AAV9-CB-Pull to minimize host immune responses against the bacterial protein. After 10 weeks, as expected, the AAV9-CB-Pull treatment showed tremendous effects in correcting glycogen accumulation in the heart and skeletal muscles but had no effect on the liver. To further restore the liver to normal structure and function, we sequentially injected these mice with a liver-restricted AAV8-LSP-Pull vector at 3 months of age. This combination treatment (CB+LSP) effectively reduced liver glycogen accumulation and recovered liver function without diminishing the effect of AAV9-CB-Pull treatment on muscles.

Biochemical clearance of glycogen storage in muscle correlates well with muscle functional improvement in the AAV-treated GSD IIIa mice. Both treadmill and Rota-rod data suggest a full restoration of muscle function by the AAV treatment. However, the wire-hang performance of the AAV-treated mice, although significantly improved compared to the untreated GSD IIIa animals, is only partially increased compared with the WT mice. This indicates that the gene therapy did not completely correct the deficits in some muscles of GSD IIIa mice related to the grasping ability of limb strength.

Unlike human GDE, Pullulanase digestion of the limit dextrin in GSD IIIa mice will create a side oligosaccharide product called maltotetraose, a linear 4-glucose molecule linked with α-1,4 glycosidic bonds. Maltotetraose is indeed a natural oligosaccharide that can be detected in normal human plasma. Oligosaccharides including maltotetraose can be hydrolyzed into glucose molecules by α-amylase and neutral glucosidases in human cells. To our knowledge, there is no report showing that this oligosaccharide is cytotoxic.

In addition to the Pullulanase used in this study, other bacterial enzymes with a similar glycogen-degrading activity can also possibly be used for GSD III gene therapy, such as type I Pullulanase derived from other bacteria species and strains[38] and the bacterial GDE encoded by the *glgX* gene in *Escherichia coli*.[39,40]

Our data suggest that Pullulanase-based gene therapy with AAV vector is a feasible treatment for GSD III. It is possible that some GSD III patients may carry point mutations that only disrupt one GDE activity while the other one remains unaffected. Pullulanase will be effective for both conditions but it may work better/faster in clearing glycogen accumulation in the patients who have no α-1,4 glucanotransferase activity. This is because Pullulanase is highly specific and active in debranching the phosphorylase-limit dextrin molecules but it still has a lower activity breaking the α-1, 6 linkages with one glucose residue in the α-1,4 glucanotransferase product.[15]

To our knowledge, this is the first report of gene therapy with a bacterial enzyme for a human disease. The same approach should be considered for other inherited diseases caused by the defect of a large human gene. However, to translate this therapeutic approach to human patients, immune responses against the bacterial enzyme need to be addressed by further studies, which are currently underway.

MATERIALS AND METHODS

Codon Optimization of Bacterial Pullulanase for Expression in Human Cells

A 2.2 kb DNA containing the codon-optimized Pullulanase cDNA (Figure S2; *Bacillus subtilis* strain 168, *amyX*, GenBank: NP_390871.2) linked with a hemagglutinin (HA)-tag sequence (5′-TACCCATACGATGTTCCAGATTACGCT-3′) at the 3′ end was synthesized and cloned into the pcDNA3.1(+) vector using KpnI and *EcoR*I sites (pcDNA3.1-Pull) at GenScript (Piscataway, NJ, USA). Pullulanase expression was verified by western blot and enzyme activity assays in HEK293T cells 48 h after transfection with the pcDNA3.1-Pull vector.

AAV Vector Constructs and Packaging

To generate the pAAV-CB-Pull vector plasmid, we subcloned the KpnI-*Eco*RI fragment containing the HA-tagged Pullulanase cDNA from the pcDNA3.1-Pull vector into the pAAV-CB-hGAA vector[41] containing the CMV enhanced chicken β-actin hybrid (CB) promoter to replace the human GAA cDNA. To generate the pAAV-LSP-Pull vector, we cloned the *Sca*I-KpnI fragment containing the liver-specific promoter (LSP) from the pAAV-LSP-hGAA vector[42] into the pAAV-CB-Pull vector to replace the CB promoter. These vectors were packaged as AAV9 (AAV9-CB-Pull) and AAV8 (AAV8-LSP-Pull) in HEK293T cells using the calcium phosphate transfection method. The viral vectors were purified using iodixanol gradient ultracentrifugation method.[43] The titer of the viral stock was determined using purified viral DNA and Southern blotting with a biotin-labeled probe generated with Prime-A-Gene labeling kit (Promega, Madison, WI, USA). The viral vector stock was handled according to Biohazard Safety Level 2 guidelines published by the National Institutes of Health.

GSD IIIa Mouse Model and Viral Vector Administration

Animal care and experiments were conducted in accordance with Duke University Institutional Animal Care and Use Committee approved guidelines. Heterozygous *Agl* mutant mice in the C57BL/6N background (C57BL/6N-$Agl^{Tm1a(EUCOMM)Wtsi}$) were purchased from the European Mouse Mutant Archive (EMMA, EMMA ID: EM05784) and crossed with the CMV-Cre mice (The Jackson Laboratory), to convert the mutant *Agl* allele into a knockout allele by deleting exons 6~10 and the neo expression cassette (Figure 1A). The resulting $Agl^{+/-}$ mice were interbred to generate homozygous

$Agl^{-/-}$ mice. $Agl^{-/-}$ mice were used as breeders to produce *Agl* knockout mice (GSD IIIa mice). For gene therapy, 2-week-old GSD IIIa mice (n = 15) were injected with AAV9-CB-Pull intravenously at a dose of 1.0×10^{13} vg/kg. At 3 months of age, 8 mice were sacrificed to collect tissues, urine, and blood and the 7 remaining mice were subsequently injected with the same dose of AAV8-LSP-Pull intravenously and sacrificed at 5 months of age to collect tissues and blood. The mice were examined for behavioral tests at 2, 2.5, 3, 4, and 5 months of age. Gender- and age-matched untreated GSD IIIa and C57BL/6J WT (from Jackson Laboratory) mice were used as controls. All the mice were fasted for 24 h prior to sacrifice to minimize the effect of normal glycogen. Fresh tissue specimens were either immediately frozen on dry ice and stored at −80°C until used for biochemical analyses or fixed immediately for histology.

AAV Vector Bio-Distribution

AAV copy number was qualified by real-time PCR.[23] Briefly, genomic DNA was extracted from frozen tissues using the Wizard Genomic DNA Purification kit (Promega, Madison, WI, USA). PCR was performed using SYBR Green (Roche, Basel, Switzerland) and the following gene-specific primer pairs: 5′-GCCACTGGATGCCTACAACT-3′ and 5′-CGTGCTGGTGCAGTGTATTG-3′ for Pullulanase and 5′-AGAGGGAAATCGTGCGTGAC-3′ and 5′-CAATAGTGATGACCTGGCCGT-3′ for mouse β-actin.[41] The pAAV-CB-Pull plasmid DNA was used to generate a standard curve for viral vector copy-number calculation.

Western Blot

Tissues were homogenized on ice in lysis buffer PBS containing 1% NP40, 0.5% sodium deoxycholate, 0.1% SDS and a protease/phosphatase inhibitor cocktail (Cell Signaling Technology, Danvers, MA, USA) using a glass homogenizer. Lysates were cleared by centrifugation at 18,000 × *g* at 4°C for 15 min. The protein concentration of the supernatants was measured using the bicinchoninic acid (BCA) assay. Equal amounts of protein were run on SDS-PAGE gels and transferred to nitrocellulose membrane. The membranes were blocked in 3% BSA/PBST, incubated with primary antibodies overnight at 4°C, washed, incubated with secondary antibodies, washed again, and developed using ECL kit (Bio-Rad, Hercules, CA, USA). The images were obtained by a ChemiDoc Image System (Bio-Rad, Hercules, CA, USA). The following antibodies were used: anti-HA (sc-805) was from Santa Cruz Biotechnology (Dallas, TX), anti-AGL (GDE; ab71423) was from Abcam (Cambridge, MA, USA), and anti-β-Actin (A3854) were from Sigma (Sigma-Aldrich, St. Louis, MO, USA).

Pullulanase Activity Assay

Pullulanase activity was measured using Pullulanase activity assay kit (Megazyme, Wicklow, Ireland) following the manufacturer's protocol. Briefly, tissues were homogenized as described above in PBS containing a protease/phosphatase inhibitor cocktail. The lysates were centrifuged at 18,000 × *g* at 4°C for 15 min. The lysates were incubated with the provided substrate (6-O-Benzylidene-4-nitrophenyl-63-α-D-maltotriosyl-maltotriose), thermostable α-glucosidase, and thermostable β-glucosidase for 10 min at 40°C. After 10 min, the reaction was stopped by adding the stop buffer (2% [w/v] Tris buffer, pH 9.0). The absorbance was read at 405 nm using a victor X multi-label plate reader (PerkinElmer Corporation, Waltham, MA, USA). Kit-provided Pullulanase enzyme was used for a standard to determine the enzyme activity. Protein concentration was determined by BCA assay and used to normalize the data.

Glycogen Content Assay

The tissues were homogenized in distilled water (1 mg of tissue/20 μL of water) using a homogenizer, followed by sonication for 15 s and centrifugation at 18,000 × g at 4°C for 15 min. The 1:5 diluted lysates were boiled for 3 min to inactivate endogenous enzymes and incubated with 0.175 U/mL (final concentration in the reaction) of Amyloglucosidase (Sigma-Aldrich, St. Louis, MO, USA) for 90 min at 37°C. The reaction mixtures were then boiled again for 3 min to stop the reaction. 30 μL of the mixtures were incubated with 1 mL of Pointe Scientific Glucose (Hexokinase) Liquid Reagents (Fisher, Hampton, NH, USA) for at least 10 min at room temperature (RT). The absorbance was read at 340 nm using a UV-VIS Spectrophotometer (Shimadzu UV-1700 PharmaSpec, Tokyo, Japan).[26]

Histology

Fresh tissues were fixed in 10% neutral-buffered formalin (NBF) for 48 h. After primary immersion fixation, the samples were post-fixed with 1% periodic acid (PA) in 10% NBF for 48 h at 4°C. The samples were then washed with PBS, dehydrated with ascending grades of alcohol, cleared with xylene, and infiltrated with paraffin. For PAS staining, sections of paraffin-embedded tissues were processed and stained using Schiff reagent as described[26,44,45] with some modifications. Briefly, the slides were oxidized with freshly made 0.5% PA for 5 min and rinsed with distilled water for 1 min. The slides were then stained with Schiff reagent for 15 min and washed with tap water for 10 min. The slides were counterstained with hematoxylin and rinsed with tap water, incubated with bluing reagent for 1 min, dehydrated, and mounted. For trichrome staining, the paraffin-embedded liver sections were processed and stained using Masson's trichrome staining kit (Sigma-Aldrich, St. Louis, MO, USA) following the manufacturer's protocol. The images were taken on a BZ-X710 microscope (Keyence America, Itasca, IL, USA).

Liver Enzyme Test in the Plasma

The activity of plasma ALT was measured using the Liquid ALT (SGPT) Reagent Set (Pointe Scientific, Canton, MI, USA) following the manufacturer's protocol. Briefly, whole blood was collected using the green blood collection tube (coated with lithium heparin) and plasma was separated by centrifugation at 2,000 × *g*, 4°C for 10 min, and diluted (1:5) with normal saline (0.9% w/v of NaCl). The diluted plasma was incubated with the working reagent (R1 and R2 mixture) at 37°C and absorbance at 340 nm was recorded every min for 5 min.

Determination of Urinary Glc4 Concentration

The concentration of urinary Glc4 was tested by stable isotope-dilution electrospray tandem mass spectrometry as previously described.[46]

Behavioral Tests

Treadmill Exhaustion Test

Mice were acclimated for 15 min in the chamber of the treadmill (LE8709, Panlab Harvard Apparatus, Holliston, MA, USA) and warmed up by running at the lowest speed, 5 cm/sec, and 25 degrees of slope for 3 min. Then, mice were allowed to run at 8 cm/sec for 3 min. The speed was increased by 4 cm/sec every 3 min until mice were exhausted or the maximal speed (32 cm/sec) was reached.

Wire Hang Test

Mice were put on the center of a wire mesh positioned 30 cm above soft bedding. The wire mesh was carefully inverted and the time until the mouse fell or the maximum time (3 min) was recorded. Three separate trials were recorded and the maximum hanging time was used for comparison.

Accelerating Rota-rod Test

Mice were acclimated to the Rota-rod[26] (ENV-577M, Med Associates, Fairfax, VT, USA) by first allowing them to stay for 3 min on the drum, which was rotating at a constant speed of four rotations per min (waiting mode). Mice were then trained twice on a gradually accelerating Rota-rod (4.0–40.0 rpm). Trained mice were then tested during three sessions using the accelerating Rota-rod protocol, and the latency to fall was recorded. This routine provided the mice at least 5 min of rest between the sessions.

Statistics

Statistical significance was determined by unpaired two-tailed Student's t test using Prism software (GraphPad, La Jolla, CA); data were presented as mean ± standard deviation (SD). *$p < 0.05$ was considered statistically significant.

SUPPLEMENTAL INFORMATION

Supplemental Information can be found online at https://doi.org/10.1016/j.omtm.2020.05.034.

AUTHOR CONTRIBUTIONS

J.L. and B.S. developed the concept, designed, performed experiments, analyzed and interpreted the data, and wrote the manuscript; S.C. and F.G. performed experiments, analyzed and interpreted the data, and participated in writing the manuscript; P.S.K. participated in analyzing the data and writing the manuscript.

CONFLICTS OF INTEREST

B.S. has received grant support from Roivant Sciences, Selecta Biosciences, Actus Therapeutics, Alnylam Pharmaceuticals, and Asklepios BioPharmaceutical (AskBio). P.S.K. has received grant support from Sanofi Genzyme, Valerion Therapeutics, Shire Pharmaceuticals, and Amicus Therapeutics. P.S.K. has received consulting fees and honoraria from Sanofi Genzyme, Shire Pharmaceuticals, Amicus Therapeutics, Vertex Pharmaceuticals, and AskBio. P.S.K. is a member of the Pompe and Gaucher Disease Registry Advisory Board for Sanofi Genzyme. P.S.K. has equity in Actus Therapeutics, which is developing gene therapy for Pompe disease. B.S., P.S.K., and J.L. are inventors of a patent application for the technology that is being used in the study. If the technology is commercially successful in the future, the developers and Duke University may benefit financially. The other authors declare no competing interests.

ACKNOWLEDGMENTS

We thank Dr. Haiqing Yi for reviewing and editing the manuscript. This work was supported by the Alice and Y.T. Chen Pediatric Genetics and Genomics Center at Duke University and by the Workman family of Lowell, Indiana.

REFERENCES

1. Taylor, C., Cox, A.J., Kernohan, J.C., and Cohen, P. (1975). Debranching enzyme from rabbit skeletal muscle. Purification, properties and physiological role. Eur. J. Biochem. *51*, 105–115.
2. Zhai, L., Feng, L., Xia, L., Yin, H., and Xiang, S. (2016). Crystal structure of glycogen debranching enzyme and insights into its catalysis and disease-causing mutations. Nat. Commun. *7*, 11229.
3. Bates, E.J., Heaton, G.M., Taylor, C., Kernohan, J.C., and Cohen, P. (1975). Debranching enzyme from rabbit skeletal muscle; evidence for the location of two active centres on a single polypeptide chain. FEBS Lett. *58*, 181–185.
4. Dagli, A., Sentner, C.P., and Weinstein, D.A. (2010). Glycogen Storage Disease Type III. In GeneReviews, M.P. Adam et al., eds. (University of Washington, Seattle).
5. Endo, Y., Horinishi, A., Vorgerd, M., Aoyama, Y., Ebara, T., Murase, T., Odawara, M., Podskarbi, T., Shin, Y.S., and Okubo, M. (2006). Molecular analysis of the AGL gene: heterogeneity of mutations in patients with glycogen storage disease type III from Germany, Canada, Afghanistan, Iran, and Turkey. J. Hum. Genet. *51*, 958–963.
6. Sentner, C.P., Hoogeveen, I.J., Weinstein, D.A., Santer, R., Murphy, E., McKiernan, P.J., Steuerwald, U., Beauchamp, N.J., Taybert, J., Laforêt, P., et al. (2016). Glycogen storage disease type III: diagnosis, genotype, management, clinical course and outcome. J. Inherit. Metab. Dis. *39*, 697–704.
7. Kishnani, P.S., Austin, S.L., Arn, P., Bali, D.S., Boney, A., Case, L.E., Chung, W.K., Desai, D.M., El-Gharbawy, A., Haller, R., et al.; ACMG (2010). Glycogen storage disease type III diagnosis and management guidelines. Genet. Med. *12*, 446–463.
8. Demo, E., Frush, D., Gottfried, M., Koepke, J., Boney, A., Bali, D., Chen, Y.T., and Kishnani, P.S. (2007). Glycogen storage disease type III-hepatocellular carcinoma a long-term complication? J. Hepatol. *46*, 492–498.
9. Halaby, C.A., Young, S.P., Austin, S., Stefanescu, E., Bali, D., Clinton, L.K., Smith, B., Pendyal, S., Upadia, J., Schooler, G.R., et al. (2019). Liver fibrosis during clinical ascertainment of glycogen storage disease type III: a need for improved and systematic monitoring. Genet. Med *21*, 2686–2694.
10. Coleman, R.A., Winter, H.S., Wolf, B., Gilchrist, J.M., and Chen, Y.T. (1992). Glycogen storage disease type III (glycogen debranching enzyme deficiency): correlation of biochemical defects with myopathy and cardiomyopathy. Ann. Intern. Med. *116*, 896–900.
11. Carvalho, J.S., Matthews, E.E., Leonard, J.V., and Deanfield, J. (1993). Cardiomyopathy of glycogen storage disease type III. Heart Vessels *8*, 155–159.
12. Vertilus, S.M., Austin, S.L., Foster, K.S., Boyette, K.E., Bali, D.S., Li, J.S., Kishnani, P.S., and Wechsler, S.B. (2010). Echocardiographic manifestations of Glycogen Storage Disease III: increase in wall thickness and left ventricular mass over time. Genet. Med. *12*, 413–423.
13. Decostre, V., Laforêt, P., De Antonio, M., Kachetel, K., Canal, A., Ollivier, G., Nadaj-Pakleza, A., Petit, F.M., Wahbi, K., Fayssoil, A., et al. (2017). Long term longitudinal study of muscle function in patients with glycogen storage disease type IIIa. Mol. Genet. Metab. *122*, 108–116.
14. Horvath, J.J., Austin, S.L., Jones, H.N., Drake, E.J., Case, L.E., Soher, B.J., Bashir, M.R., and Kishnani, P.S. (2012). Bulbar muscle weakness and fatty lingual infiltration in glycogen storage disorder type IIIa. Mol. Genet. Metab. *107*, 496–500.
15. Shim, J.H., Park, J.T., Hong, J.S., Kim, K.W., Kim, M.J., Auh, J.H., Kim, Y.W., Park, C.S., Boos, W., Kim, J.W., and Park, K.H. (2009). Role of maltogenic amylase and

pullulanase in maltodextrin and glycogen metabolism of Bacillus subtilis 168. J. Bacteriol. *191*, 4835–4844.

16. Yi, H., Thurberg, B.L., Curtis, S., Austin, S., Fyfe, J., Koeberl, D.D., Kishnani, P.S., and Sun, B. (2012). Characterization of a canine model of glycogen storage disease type IIIa. Dis. Model. Mech. *5*, 804–811.
17. Young, S.P., Zhang, H., Corzo, D., Thurberg, B.L., Bali, D., Kishnani, P.S., and Millington, D.S. (2009). Long-term monitoring of patients with infantile-onset Pompe disease on enzyme replacement therapy using a urinary glucose tetrasaccharide biomarker. Genet. Med. *11*, 536–541.
18. Sluiter, W., van den Bosch, J.C., Goudriaan, D.A., van Gelder, C.M., de Vries, J.M., Huijmans, J.G., Reuser, A.J., van der Ploeg, A.T., and Ruijter, G.J. (2012). Rapid ultra-performance liquid chromatography-tandem mass spectrometry assay for a characteristic glycogen-derived tetrasaccharide in Pompe disease and other glycogen storage diseases. Clin. Chem. *58*, 1139–1147.
19. Brooks, E.D., Yi, H., Austin, S.L., Thurberg, B.L., Young, S.P., Fyfe, J.C., Kishnani, P.S., and Sun, B. (2016). Natural Progression of Canine Glycogen Storage Disease Type IIIa. Comp. Med. *66*, 41–51.
20. Aartsma-Rus, A., and van Putten, M. (2014). Assessing functional performance in the mdx mouse model. J. Vis. Exp. *85*, 51303.
21. Castro, B., and Kuang, S. (2017). Evaluation of Muscle Performance in Mice by Treadmill Exhaustion Test and Whole-limb Grip Strength Assay. Biol. Protoc *7*, e2237.
22. Bonetto, A., Andersson, D.C., and Waning, D.L. (2015). Assessment of muscle mass and strength in mice. Bonekey Rep. *4*, 732.
23. Liu, K.M., Wu, J.Y., and Chen, Y.T. (2014). Mouse model of glycogen storage disease type III. Mol. Genet. Metab. *111*, 467–476.
24. Pagliarani, S., Lucchiari, S., Ulzi, G., Violano, R., Ripolone, M., Bordoni, A., Nizzardo, M., Gatti, S., Corti, S., Moggio, M., et al. (2014). Glycogen storage disease type III: A novel Agl knockout mouse model. Biochim. Biophys. Acta *1842*, 2318–2328.
25. Vidal, P., Pagliarani, S., Colella, P., Costa Verdera, H., Jauze, L., Gjorgjieva, M., Puzzo, F., Marmier, S., Collaud, F., Simon Sola, M., et al. (2018). Rescue of GSDIII Phenotype with Gene Transfer Requires Liver- and Muscle-Targeted GDE Expression. Mol. Ther. *26*, 890–901.
26. Lim, J.A., Yi, H., Gao, F., Raben, N., Kishnani, P.S., and Sun, B. (2019). Intravenous Injection of an AAV-PHP.B Vector Encoding Human Acid α-Glucosidase Rescues Both Muscle and CNS Defects in Murine Pompe Disease. Mol. Ther. Methods Clin. Dev. *12*, 233–245.
27. Michon, C.C., Gargiulo, M., Hahn-Barma, V., Petit, F., Nadaj-Pakleza, A., Herson, A., Eymard, B., Labrune, P., and Laforet, P. (2015). Cognitive profile of patients with glycogen storage disease type III: a clinical description of seven cases. J. Inherit. Metab. Dis. *38*, 573–580.
28. Sentner, C.P., Caliskan, K., Vletter, W.B., and Smit, G.P. (2012). Heart Failure Due to Severe Hypertrophic Cardiomyopathy Reversed by Low Calorie, High Protein Dietary Adjustments in a Glycogen Storage Disease Type IIIa Patient. JIMD Rep. *5*, 13–16.
29. Pagliarani, S., Lucchiari, S., Ulzi, G., Ripolone, M., Violano, R., Fortunato, F., Bordoni, A., Corti, S., Moggio, M., Bresolin, N., and Comi, G.P. (2018). Glucose-free/high-protein diet improves hepatomegaly and exercise intolerance in glycogen storage disease type III mice. Biochim. Biophys. Acta Mol. Basis Dis. *1864*, 3407–3417.
30. Sun, B., Fredrickson, K., Austin, S., Tolun, A.A., Thurberg, B.L., Kraus, W.E., Bali, D., Chen, Y.T., and Kishnani, P.S. (2013). Alglucosidase alfa enzyme replacement therapy as a therapeutic approach for glycogen storage disease type III. Mol. Genet. Metab. *108*, 145–147.
31. Yi, H., Brooks, E.D., Thurberg, B.L., Fyfe, J.C., Kishnani, P.S., and Sun, B. (2014). Correction of glycogen storage disease type III with rapamycin in a canine model. J. Mol. Med. (Berl.) *92*, 641–650.
32. Pursell, N., Gierut, J., Zhou, W., Dills, M., Diwanji, R., Gjorgjieva, M., Saxena, U., Yang, J.S., Shah, A., Venkat, N., et al. (2018). Inhibition of Glycogen Synthase II with RNAi Prevents Liver Injury in Mouse Models of Glycogen Storage Diseases. Mol. Ther. *26*, 1771–1782.
33. Inagaki, K., Fuess, S., Storm, T.A., Gibson, G.A., Mctiernan, C.F., Kay, M.A., and Nakai, H. (2006). Robust systemic transduction with AAV9 vectors in mice: efficient global cardiac gene transfer superior to that of AAV8. Mol. Ther. *14*, 45–53.
34. Zincarelli, C., Soltys, S., Rengo, G., and Rabinowitz, J.E. (2008). Analysis of AAV serotypes 1-9 mediated gene expression and tropism in mice after systemic injection. Mol. Ther. *16*, 1073–1080.
35. Jacobs, F., and Wang, L. (2011). Adeno-associated viral vectors for correction of inborn errors of metabolism: progressing towards clinical application. Curr. Pharm. Des. *17*, 2500–2515.
36. Dayton, R.D., Wang, D.B., and Klein, R.L. (2012). The advent of AAV9 expands applications for brain and spinal cord gene delivery. Expert Opin. Biol. Ther. *12*, 757–766.
37. Nathwani, A.C., Reiss, U.M., Tuddenham, E.G., Rosales, C., Chowdary, P., McIntosh, J., Della Peruta, M., Lheriteau, E., Patel, N., Raj, D., et al. (2014). Long-term safety and efficacy of factor IX gene therapy in hemophilia B. N. Engl. J. Med. *371*, 1994–2004.
38. Michaelis, S., Chapon, C., D'Enfert, C., Pugsley, A.P., and Schwartz, M. (1985). Characterization and expression of the structural gene for pullulanase, a maltose-inducible secreted protein of Klebsiella pneumoniae. J. Bacteriol. *164*, 633–638.
39. Jeanningros, R., Creuzet-Sigal, N., Frixon, C., and Cattaneo, J. (1976). Purification and properties of a debranching enzyme from Escherichia coli. Biochim. Biophys. Acta *438*, 186–199.
40. Dauvillée, D., Kinderf, I.S., Li, Z., Kosar-Hashemi, B., Samuel, M.S., Rampling, L., Ball, S., and Morell, M.K. (2005). Role of the Escherichia coli glgX gene in glycogen metabolism. J. Bacteriol. *187*, 1465–1473.
41. Sun, B., Chen, Y.T., Bird, A., Xu, F., Hou, Y.X., Amalfitano, A., and Koeberl, D.D. (2003). Packaging of an AAV vector encoding human acid alpha-glucosidase for gene therapy in glycogen storage disease type II with a modified hybrid adenovirus-AAV vector. Mol. Ther. *7*, 467–477.
42. Franco, L.M., Sun, B., Yang, X., Bird, A., Zhang, H., Schneider, A., Brown, T., Young, S.P., Clay, T.M., Amalfitano, A., et al. (2005). Evasion of immune responses to introduced human acid alpha-glucosidase by liver-restricted expression in glycogen storage disease type II. Mol. Ther. *12*, 876–884.
43. Lock, M., Alvira, M., Vandenberghe, L.H., Samanta, A., Toelen, J., Debyser, Z., and Wilson, J.M. (2010). Rapid, simple, and versatile manufacturing of recombinant adeno-associated viral vectors at scale. Hum. Gene Ther. *21*, 1259–1271.
44. Lynch, C.M., Johnson, J., Vaccaro, C., and Thurberg, B.L. (2005). High-resolution light microscopy (HRLM) and digital analysis of Pompe disease pathology. J. Histochem. Cytochem. *53*, 63–73.
45. Taksir, T.V., Griffiths, D., Johnson, J., Ryan, S., Shihabuddin, L.S., and Thurberg, B.L. (2007). Optimized preservation of CNS morphology for the identification of glycogen in the Pompe mouse model. J. Histochem. Cytochem. *55*, 991–998.
46. Young, S.P., Stevens, R.D., An, Y., Chen, Y.T., and Millington, D.S. (2003). Analysis of a glucose tetrasaccharide elevated in Pompe disease by stable isotope dilution-electrospray ionization tandem mass spectrometry. Anal. Biochem. *316*, 175–180.